# Two-Parameter Locus of Boundary Crisis: Mind the Gaps!

Hinke M. Osinga and James Rankin

Bristol Centre for Applied Nonlinear Mathematics,
Department of Engineering Mathematics,
University of Bristol, Queen's Building, Bristol BS8 1TR, UK

Preprint of July 2010

**Abstract**

Boundary crisis is a mechanism for destroying a chaotic attractor when one parameter is varied. In a two-parameter setting the locus of boundary crisis is associated with curves of homo- or heteroclinic tangency bifurcations of saddle periodic orbits. It is known that the locus of boundary crisis contains many gaps, corresponding to channels (regions of positive measure) where a non-chaotic attractor persists. One side of such a subduction channel is a saddle-node bifurcation of a periodic orbit that marks the start of a periodic window in the chaotic regime; the other side of the channel is formed by a homo- or heteroclinic tangency bifurcation associated with this diffferent saddle periodic orbit. We present a two-parameter study of boundary crisis in the Ikeda map, which models the dynamics of energy levels in a laser ring cavity. We confirm the existence of many gaps on the boundary-crisis locus. However, the gaps correspond to subduction channels that can have a rather different structure compared to what is known in the literature.

## 1 Introduction

The Ikeda map [12, 13] models the behaviour of a laser ring cavity system, which is a series of mirrors forming a ring around which light is reflected. The ring cavity receives input from a laser and light is recirculated through an absorber in the cavity. The Ikeda map $F : \mathbb{C} \to \mathbb{C}$ describes the changes in the complex field amplitude $g \in \mathbb{C}$ after each round trip through the ring cavity. We use the definition as given in [5, 11], that is,

$$F(g) := a + R\,g\,\exp\left[i\left(\phi - \frac{p}{1+|g|^2}\right)\right], \tag{1}$$

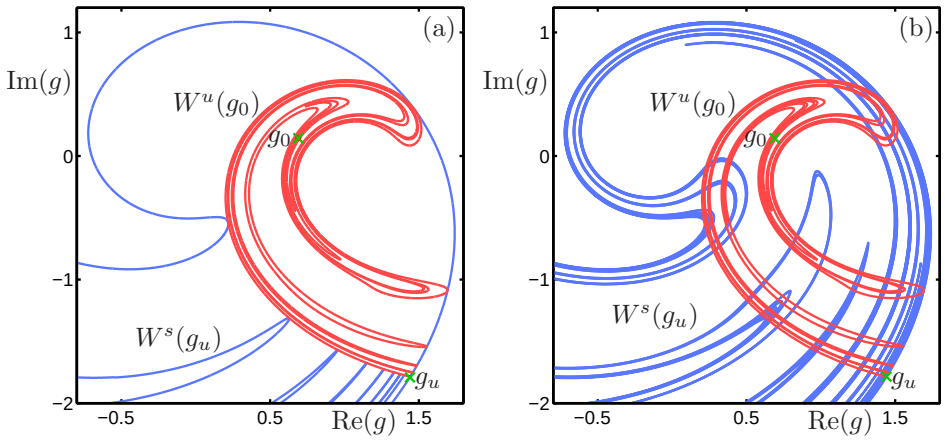


Figure 1: Boundary crisis in the Ikeda map (1) with $R = 0.784$ and $a \approx 1.222671$ is due to a tangency between the unstable and stable manifolds $W^u(g_0)$ and $W^s(g_u)$ of the fixed points $g_0$ and $g_u$, respectively. The approximate tangency is shown in panel (a) and panel (b) shows the heteroclinic tangle for $a = 1.2227$, for which the chaotic attractor has disappeared and all initial conditions eventually converge to the fixed-point attractor $g_\infty$ (not shown).

where $a > 0$ represents the amplitude of the laser input, $0 < R < 1$ is the scaled reflectivity of the mirrors, $\phi$ is the cavity detuning parameter, and $p$ is an additional detuning parameter when a nonlinear medium is present. Under normal circumstances, the laser ring cavity transmits coherent light, which corresponds to a fixed point or periodic orbit of the Ikeda map (1). If the energy levels in the ring cavity change chaotically then the transmitted light is still coherent but the frequency spectrum is broad as for an ordinary incandescent light source. Previous studies have shown that the Ikeda map can have a co-existing chaotic attractor [4, 11]; in such parameter regimes it is important to understand the transitions from "safe" steady behaviour to chaotic dynamics. In particular, parameter variations can lead to the sudden appearance or sudden change in size of a chaotic attractor. These phenomena are known as *crisis bifurcations* and are the focus of this paper. Throughout this study, we vary the amplitude $a$ and reflectivity $R$, while keeping the detunings $\phi$ and $p$ fixed at the physically relevant values 0.4 and 6.0, respectively.

Crisis bifurcations were first identified in 1979 [22, 23] and are known to occur in the Ikeda map [5]. We are primarily interested in boundary crisis, which causes the sudden appearance (or disappearance) of a chaotic attractor as a parameter is varied. As discussed in [5], under two-parameter variations, boundary crisis interacts with the other two crisis bifurcations, namely, interior crisis and basin boundary metamorphisis, which cause sudden changes in the sizes of the attractor and its basin of attraction, respectively. Crisis bifurcations are different manifestations of a homo- or heteroclinic tangency between the global (un)stable manifolds of the same or two different periodic orbits, respectively [7, 8, 9]; the type of crisis

that occurs depends on whether the attractor is actually chaotic and whether (one of) the periodic orbits lies on the boundary or in the interior of its basin of attraction. Figure 1 illustrates a boundary crisis for the Ikeda map (1) with $R = 0.784$ and $a \approx 1.222671$. Just before the boundary crisis the chaotic attractor and the global unstable manifold $W^u(g_0)$ of a saddle fixed point $g_0$ have the same closure. The global stable manifold $W^s(g_u)$ of another fixed point $g_u$ separates the basins of this attractor and a third attracting fixed point $g_\infty$. As soon as $W^u(g_0)$ and $W^s(g_u)$ are tangent, the chaotic attractor disappears and its basin is absorbed by the basin of $g_\infty$; Fig. 1(a) illustrates the tangency between $W^u(g_0)$ and $W^s(g_u)$. After the boundary crisis, a chaotic saddle remains that gives rise to long chaotic transients; this chaotic saddle is formed by a heteroclinic tangle, as shown in Fig. 1(b) for $a = 1.2227$.

Tangencies of global manifolds are structurally stable in a two-parameter setting and the tangency locus forms a smooth curve in the parameter plane [18]. Therefore, one might expect that a similarly smooth curve can be identified as a crisis locus. The locus of boundary crisis has been studied extensively with the example of the Hénon map [10]. In [5] a piecewise-smooth curve in the parameter plane is identified as the boundary between chaotic dynamics and divergence, with periodic behaviour existing only as part of the transition to chaos in the chaotic regime. The non-differentiable points on the locus of boundary crisis are known as *double-crisis vertices*. As explained in [5], a double-crisis vertex $V$ is the intersection point of two smooth curves that correspond to two different tangency loci; each tangency locus has a segment ending at $V$ that gives rise to a boundary crisis, but the other segments ending at $V$ correspond to an interior crisis for one of the tangency loci and a basin boundary metamorphosis for the other. The study in [5] seems to suggest that the different loci of boundary crises form a single connected piecewise-smooth curve. However, there are many, possibly infinitely many, gaps that give rise to subduction channels transverse to the crisis locus, inside which the dynamics is periodic [16, 17]. One of the end points of such a gap is a double-crisis vertex, but the other lies on the locus of a saddle-node bifurcation in the parameter plane, which organises the onset of a periodic window in the chaotic regime. Hence, for the Hénon map, each channel is bounded on one side by a curve of saddle-node bifurcations and contains an accumulating family of curves that correspond to period-doubling sequences to chaos; the chaotic attractors disappear in a boundary crisis on the other side of the channel. We say that such a channel is of subduction-crisis type.

In this paper we study the loci of boundary crisis for the Ikeda map (1) in the $(a, R)$-plane. While the overall structure of the crisis loci is similar to that of the Hénon map [10, 16, 17], we find that the channels are not necessarily of subduction-crisis type. A more complex organisation emerges that we believe should be considered as typical for two-dimensional dissipative maps. In what follows we use a brute-force numerical method to identify and characterise the attractors and overlay the results with curves of saddle-node and period-doubling bifurcations obtained by continuation with CONTENT [6]. The tangency loci of the global (un)stable manifolds involved in the crisis bifurcations were computed numerically with the extension package GM1D [3, 14] that needs DSTOOL [1].

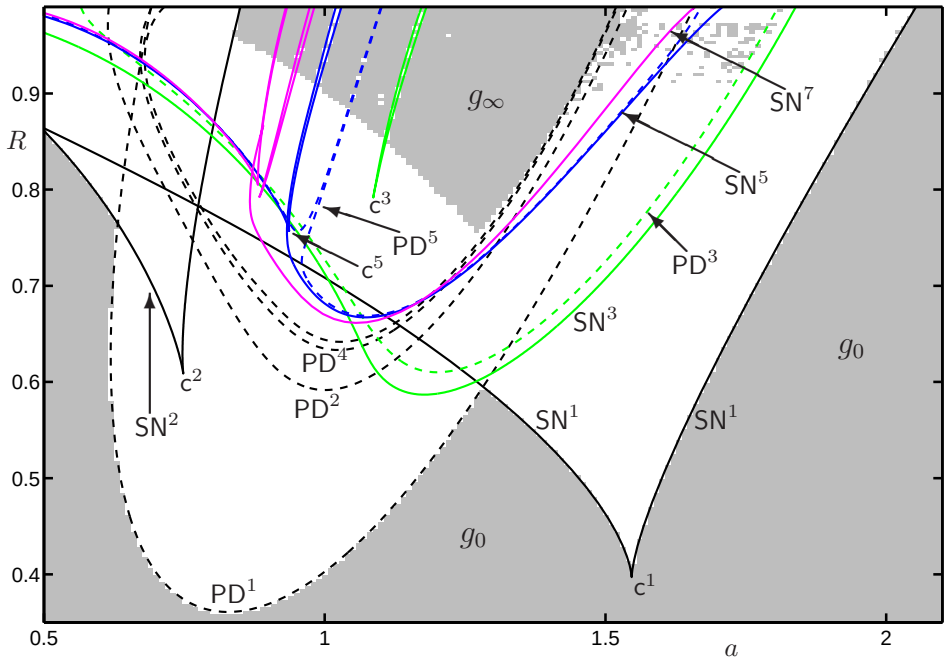


Figure 2: Iterates of 5000 initial conditions, using a grid of 40,000 parameter values, identify regions with only fixed-point attractors (grey). Overlayed are curves of saddle-node (solid, labelled SN) and period-doubling bifurcations (dashed, labelled PD); cusp points are labelled c. The superscript indicates the period of the periodic orbits involved; shown are curves for fixed points (black), and periodic orbits with periods three (green), five (blue) and seven (magenta).

## 2 Two-parameter investigation of the Ikeda map

We describe the behaviour of the Ikeda map (1) in dependence on the two parameters $a > 0$ and $0 < R < 1$. From the analysis in [11], we know that the Ikeda map can have at most three fixed points. A curve $\mathsf{SN}^1$ of saddle-node bifurcations of fixed points exist in $(a, R)$-space, which has a cusp point $\mathsf{c}^1$ at $(a, R) \approx (1.547, 0.398)$. For values of $(a, R)$ below $\mathsf{SN}^1$ there is only one fixed point, denoted $g_0$; above $\mathsf{SN}^1$ an additional two fixed points exist, denoted $g_u$ (which is always a saddle) and $g_\infty$. For $R$ small enough and/or $a$ large enough $g_0$ is an attractor and no other attractors exist. The region of parameter space with predominantly non-trivial dynamics is contained inside the box $\{(a, R) \in [0, 2.1] \times [0.35, 1]\}$ and we restrict our attention to this parameter region only.

Figure 2 illustrates the regions in the $(a, R)$-plane where a single fixed-point attractor exists; we identified these regions with trivial dynamics, which are shaded grey, using a grid of 40,000 points in the parameter plane and iterating 5000 initial conditions for each $(R, a)$-parameter pair. Overlayed in Fig. 2 are several bifurcation curves found by numerical

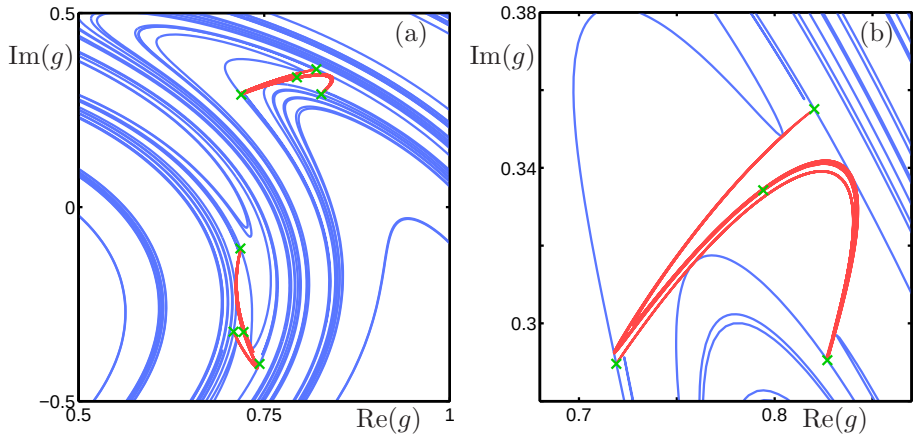


Figure 3: Boundary crisis in the Ikeda map (1) with $R = 0.784$ and $a \approx 1.3162$ is due to a tangency between the unstable manifold of a period-two orbit and the stable manifold of a period-six orbit. Panel (b) shows an enlargement of one of the two pieces of the attractor.

continuation. In particular, the curve of saddle-node bifurcations $\mathsf{SN}^1$ bounds a region with three co-existing fixed points. The curve $\mathsf{SN}^1$ is the boundary of the regime with $g_0$ as the only attractor if $a$ is large, and also if $a$ is very small (not shown). Approximately for $a > 0.5$ this boundary is formed by the curve $\mathsf{SN}^2$ of saddle-node bifurcations of period-two orbits or, as $a$ increases, the period-doubling bifurcation curve $\mathsf{PD}^1$; in both cases an attracting period-two orbit appears. Note that $g_0$ remains a stable fixed point across $\mathsf{SN}^1$ or $\mathsf{SN}^2$, but loses stability at $\mathsf{PD}^1$.

The curve $\mathsf{PD}^1$ is the first in an infinite series of period-doubling bifurcations that result in the creation of a chaotic attractor; the curves $\mathsf{PD}^2$, $\mathsf{PD}^4$ and $\mathsf{PD}^8$ (not labelled) are shown in Fig. 2. We call this chaotic attractor the principal chaotic attractor, as it is the focus of the study by Gallas *et al.* [5], who investigated the small region $(a, R) \in [1.2, 1.38] \times [0.74, 0.8]$. A double-crisis vertex exists at $(a, R) \approx (1.275, 0.754)$ on a wedge-shaped crisis locus; in Fig. 2 it is the minimum of the grey region in which $g_\infty$ is the only attractor. Along the left boundary of the wedge, the boundary crisis is mediated by a tangency between $W^u(g_0)$ and $W^s(g_u)$, as illustrated in Fig. 1; the principal chaotic attractor exists for smaller $a$ and consists of a single piece. Along the right boundary of the wedge, the boundary crisis is mediated by a tangency between the global unstable manifold of a period-two orbit and the global stable manifold of a period-six orbit on the basin boundary; this is illustrated in Fig. 3 for $(a, R) = (1.3162, 0.784)$, and we see that the principal chaotic attractor, which exists for larger $a$, consists of two pieces. The top-left boundary of the region where $g_\infty$ is the only attractor is formed by the curve $\mathsf{SN}^2$. We remark that the grey patches in Fig. 2 for $a > 1.5$ and $R$ close to 1 are probably not accurate and other attractors coexist, but with very small basins of attraction; we did not investigate this further.

The other curves in Fig. 2 correspond to saddle-node and period-doubling bifurcations of periodic orbits with periods three, five and seven; the curves for higher-periodic orbits are expected to show a similar structure. Each curve $\mathsf{N}^k$, for some positive integrer $k$, gives rise to a period-$k$ attractor that also undergoes a period-doubling sequence to chaos, starting with $\mathsf{PD}^k$. The resulting $k$-piece chaotic attractor eventually disappears; this can be due to an interior crisis, which happens if $\mathsf{N}^k$ is the start of a periodic window for the principal chaotic attractor, or a boundary crisis if there is no principal chaotic attractor. We remark here that the attractor originating from the curve labelled $\mathsf{SN}^3$ in Fig. 2 is not associated with a periodic window; this three-piece chaotic attractor co-exists with the principal chaotic attractor and always disappears in a boundary crisis.

At first glance, the bifurcation diagram shown in Fig. 2 is very similar to that for the Hénon map [10], which was studied in detail in [16, 17]. The bifurcation curves that extend into the wedge-shaped region, for which $g_\infty$ is the only attractor, are periodic windows, or subduction channels, that cross the locus of boundary crisis; this can be seen, in particular, for the crisis locus related to the tangency between $W^u(g_0)$ and $W^s(g_u)$. We found that the channels for the Ikeda map (1) are not necessarily of subduction-crisis type, as are all of those identified in the literature so far. We discuss the structures for the periodic orbits with periods three, five and seven in detail in the next section.

# 3 The structure of the subduction channels

All subduction channels of the Hénon map [10] appear to have the same structure [16, 17]. They are all of subduction-crisis type and the relative ordering of the curves $\mathsf{SN}^k$ and $\mathsf{PD}^k$ on a particular crisis locus is the same for all $k$. We computed an approximation of the two loci of tangengies between $W^u(g_0)$ and $W^s(g_u)$ and between the manifolds of the period-two and -six orbits; the enlargement in Fig. 4 shows that the tangency loci closely fit the data obtained from iterating initial conditions. From now on, we focus exclusively on interactions with the tangency locus of $W^u(g_0)$ and $W^s(g_u)$, which we call $\mathsf{BC}_1$, but similar phenomena occur for the other tangency loci.

Figure 4 clearly shows how saddle-node and period-doubling bifurcation curves cross $\mathsf{BC}_1$ transversely. The curves labelled $\mathsf{SN}^3$, $\mathsf{SN}^5$ and $\mathsf{PD}^5$ clearly bound subduction channels (white) that protrude into the region past the crisis locus (grey), but the structure is different from that found in the Hénon map. For example, Fig. 4 shows a subduction channel bounded entirely by a curve $\mathsf{SN}^3$ and one bounded entirely by $\mathsf{SN}^5$. What is more, there appears to be a channel bounded by two curves $\mathsf{PD}^5$ of period-doubling bifurcations of period-five points; these channels are not of subduction-crisis type. Let us discuss the structure of each of these channels in order, starting with the lowest period.

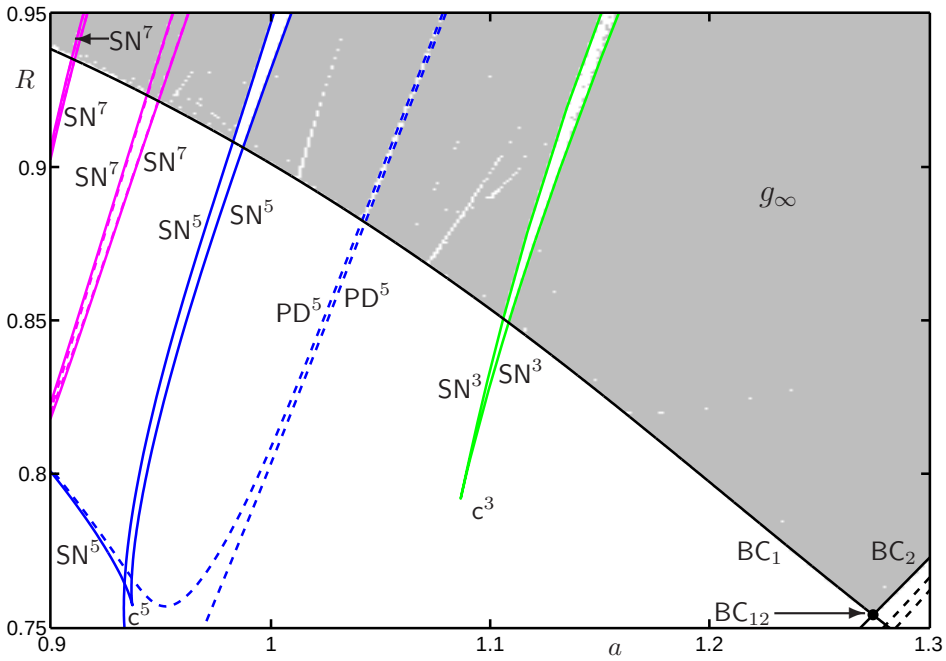


Figure 4: Enlargement of Fig. 2 illustrating part of the crisis locus. The black curves labelled $\mathsf{BC}_1$ and $\mathsf{BC}_2$ are approximations of the tangency loci that mediate the boundary crisis; they intersect at $\mathsf{BC}_{12}$, which is the double-crisis vertex at $(a, R) \approx (1.275, 0.754)$. The crisis locus $\mathsf{BC}_1$ is interspersed with gaps where non-trivial dynamics persists into the grey region. The gaps are formed by transverse intersections of saddle-node (solid) and period-doubling (dashed) bifurcations, of which those for orbits with periods three, five and seven are labelled.

## 3.1 Subduction channels organised by period-three orbits

We already mentioned the lower saddle-node curve $\mathsf{SN}^3$ shown in Fig. 2 with the nearby period-doubling curve $\mathsf{PD}^3$. These curves are part of the creation of a three-piece chaotic attractor that co-exists with the attracting fixed point $g_0$ and disappears in a boundary crisis. The curve $\mathsf{SN}^3$ that bounds a subduction channel in Fig. 4 is a separate saddle-node curve of period-three orbits that has a cusp point $\mathsf{c}^3$ at $(a, R) \approx (1.087, 0.793)$. In contrast to the curve $\mathsf{SN}^1$ in Fig. 2, which gives rise to the co-existing attracting fixed points $g_0$ and $g_\infty$ inside the cusped wedge, $\mathsf{SN}^3$ only gives rise to an attracting period-three orbit inside the channel formed by $\mathsf{SN}^3$, and the other period-three orbits are of saddle type; this is the period-three saddle formed in the saddle-node bifurcation of the lower curve $\mathsf{SN}^3$. In the regime where the principal chaotic attractor exists, this channel forms a period-three periodic window with no further period-doubling bifurcations. Therefore, we say that this channel of subduction-subduction type. The segment of $\mathsf{BC}_1$ inside the channel corresponds to a basin boundary metamorphisis that drastically reduces the basin of attraction of the period-three attractor, which co-exists with $g_\infty$.

We remark here that the bifurcation structure for the period-three orbits is different from the so-called *crossroad area* bifurcation structure that is expected to occur in two-dimensional maps with period-doubling cascades and which is so typical for the Hénon map [10, 16, 17]; see [2, 15] for further details. While the observed deviations from the crossroad area are equally generic structures, it is precisely the difference in relative locations of the bifurcation curves that causes the differences in types of the subduction channels.

## 3.2 Subduction channels organised by period-five orbits

Figure 4 shows that there are two channels across $\mathsf{BC}_1$ that are associated with period-five orbits. Note that the period-doubling bifurcation curves $\mathsf{PD}^5$ are shifted with respect to the cusp point $\mathsf{c}^5$, which lies at $(a, R) \approx (0.937, 0.757)$, in a way that is quite different from the standard crossroad area structure. The only part that is similar is the combination of the curves $\mathsf{SN}^5$ and $\mathsf{PD}^5$ to the left of $\mathsf{c}^5$; here, $\mathsf{SN}^5$ gives rise to a periodic window for the principal chaotic attractor and the nearby curve $\mathsf{PD}^5$ is the first of a period-doubling sequence to a five-piece chaotic attractor that ends in an interior crisis bifurcation. The other parts of these curves in Fig. 4 give rise to two subduction channels that are clearly not of the same type.

Let us first consider the period-five channel bounded by $\mathsf{SN}^5$. This channel is formed by two disjoint curves $\mathsf{SN}^5$, but the situation gives rise to a channel of subduction-subduction type in much the same way as for the period-three case; a period-five attractor exists only inside the channel and disappears on either side of the channel in a saddle-node bifurcation with one of the two co-existing period-five saddles. Note that co-existing period-five attractors do exist in the region near $\mathsf{c}^5$ in Fig. 4.

The period-five channel bounded by the curves $\mathsf{PD}^5$ in Fig. 4 contains an attracting

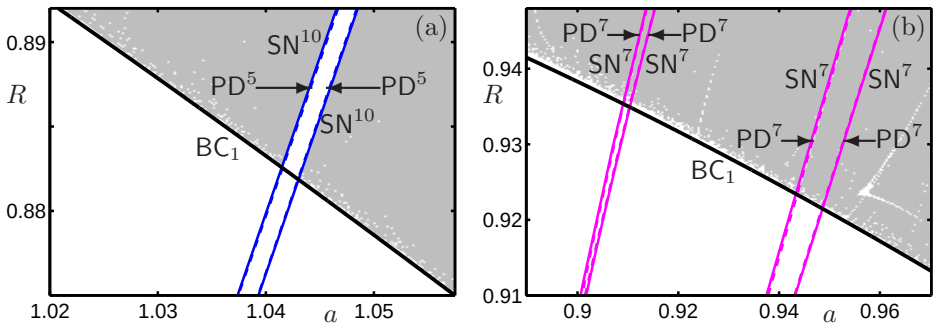


Figure 5: Detail of period-five (a) and period-seven (b) subduction channels; the two curves $\mathsf{PD}^5$ lie inside a subduction-subduction channel bounded by two curves $\mathsf{SN}^{10}$ of saddle-node bifurcations of period-ten orbits, but the attractor inside this channel has period five. There are four period-seven channels shown, which are all of subduction-crisis type.

period-five orbit. The period-doubling bifurcations are both supercritical so that an attracting period-ten orbit exists on either side of the channel, where the period-five orbit is unstable. Indeed, the subduction channel is actually slightly wider and bounded by saddle-node bifurcation curves of period-ten orbits. A further enlargement in Fig. 5(a) shows these two curves $\mathsf{SN}^{10}$. Hence, this channel is of subduction-subduction type, as before, but with additional period-doubling bifurcations inside that reduce the period of the attractor.

### 3.3 Subduction channels organised by period-seven orbits

Figure 5(b) shows further details of the period-seven subduction channels. There are four period-seven channels that are all of subduction-crisis type. However, there is a difference with the structure of period-seven channels observed for the Hénon map [10, 16, 17]. Namely, the first and third period-seven channels shown in Fig. 5(b) are bounded on the left by curves $\mathsf{SN}^7$ followed by period-doubling sequences to period-seven attractors that disappear in a boundary crisis at the right boundary of these channels; the second and fourth period-seven channels, on the other hand, are bounded on the right by curves $\mathsf{SN}^7$ and the boundary crisis occurs at the left boundaries. For the Hénon map such pairwise mirror-image channels do not occur on the same crisis locus; compare, for example, [17, Figure 6(d)].

## 4 Discussion

We studied boundary crisis bifurcations [7] of the Ikeda map (1) in dependence on the two parameters $a > 0$ and $0 < R < 1$, which represent the amplitude of the laser input and the scaled reflectivity of the mirrors in a laser ring cavity model, respectively. As expected from earlier studies of the Hénon map, boundary crisis does not depend smoothly on parameters.

Smooth curves are obtains as the loci of tangencies between smooth manifolds of periodic orbits, but only a (possibily infinite) collection of finite-length segments of the tangency loci correspond to boundary crisis bifurcations; the other segments correspond to interior crisis or basin boundary metamorphosis bifurcations.

Boundary crisis in the Ikeda map has been considered before by Gallas *et al.* [5], who only showed that the crisis locus contains at least one double-crisis vertex at which the tangency locus of the stable and unstable manifolds of a fixed point meet the tangeny locus of the stable manifold of a period-two orbit and the unstable manifold of a period-six orbit; these two tangency loci are denoted $\mathsf{BC}_1$ and $\mathsf{BC}_2$ in this paper, respectively. We studied the structure of the gaps along the tangency locus $\mathsf{BC}_1$ that do not correspond to boundary crisis. Gallas *et al.* [5] already mentioned the existence of such gaps, but did not investigate their meaning. The gaps are associated with subduction channels transverse to the tangency locus.

Our study complements the findings for the Hénon map [16, 17], where the subduction channels are all of subduction-crisis type. For example, a subduction channel asscoiated with a periodic orbit of period $k \in \mathbb{N}$ is bounded on one side by a curve of saddle-node bifurcations of $k$-periodic orbits; inside the channel a period-doubling cascade with base $k$ occurs, and the other side of the channel is bounded by a tangency locus of manifolds of a period-$k$ orbit that leads to boundary crisis of a $k$-piece chaotic attractor in the regions where the attractor is periodic. In fact, the 'orientation' of the subduction channels, that is, the relative ordering of the saddle-node, period-doubling and homoclinic (or heteroclinic) bifurcations are all the same along a tangency locus. We found that such a nice ordered structure is not present in the Ikeda map; the subduction channels are not necessarily of subduction-crisis type and the orientation may be reversed for channels crossing the same crisis locus.

We considered subduction channels in the Ikeda map that arise from saddle-node bifurcations of periodic orbits with periods 3, 5 and 7. Even for these relatively low periods, we already found a wide range of different types of subduction channels. The Ikeda map has a period-3 subduction channel that contains an attractor that coexists with the primary attractor arising from the fixed point $g_0$. Hence, the saddle-node bifurcation of the period-three orbit that marks one side of this channel never gives rise to a periodic window. Coexisting attractors are also known to exist for the Hénon map, but it appears that there is always a parameter regime where interactions between the attractors occur [19]. The period-3 subduction channel that crosses $\mathsf{BC}_1$ transversely does form a periodic window for the primary chaotic attractor, but the channel does not contain a period-doubling cascade. Similarly, the period-5 subduction channel does not contain period-doubling bifurcations in the neighbourhood of $\mathsf{BC}_1$, but two period-5-doubling bifurcation curves form another subduction channel that turns out to be bounded by two saddle-node bifurcations of a period-ten orbit. There are no crisis bifurcations associated with these channels, except for the basin boundary metamorphosis bifurcation that occurs at $\mathsf{BC}_1$. The period-7 subduction channels that we found are all of subduction-crisis type, but they occur in pairs and the ordering

of the saddle-node and period-doubling bifurcations for one of the channels in each pair is reversed.

Recent work by Sander and Yorke [20, 21] shows that there are typically infinitely many period-doubling cascades for a one- or two-dimensional map as soon as there is one. This means, in particular, that one must expect infinitely many periodic windows under one-parameter variation of a chaotic attractor and, thus, there are infinitely many gaps along the associated boundary crisis loci. Furthermore, period-doubling cascades may occur in pairs that are connected via a common saddle periodic orbit [21]; such pairs may be destroyed if a different parameter is varied. We believe that our pairs of period-7 subduction channels arise from such paired period-doubling cascades and their structure may well change as another parameter is varied; in fact, such paired channels could merge and form channels of subduction-subduction type, as we found for the period-3 and period-5 orbits. A more detailed three-parameter study of these channels will be reported elsewhere.

# Acknowledgments

The research of HMO was supported by an Advanced Research Fellowship from the Engineering and Physical Sciences Research Council. The research of JR was supported by the Natural Environment Research Council.

# References

[1] A. Back, J. Guckenheimer, M.R. Myers, F.J. Wicklin and P.A. Worfolk, *DsTool: Computer assisted exploration of dynamical systems*, Notices of the American Mathematical Society, **39**(4) (1992), 303–309.

[2] J.-P. Carcassès, C. Mira, M. Bosch, C. Simó and J.C. Tatjer, *"Crossroad area-spring area" transition I. Parameter plane representation*, Int. J. Bifurcation & Chaos **1**(1) (1991), 183–196.

[3] J.P. England, B. Krauskopf and H.M. Osinga, *Computing one-dimensional stable manifolds of planar maps without the inverse*, SIAM J. Applied Dynamical Systems, **3**(2) (2004), 161–190.

[4] Z. Galias, *Rigorous investigation of the Ikeda map by means of interval arithmetic*, Nonlinearity, **15** (2002), 1759–1779.

[5] J.A. Gallas, C. Grebogi and J.A. Yorke, *Vertices in parameter space: double crises which destroy chaotic attractors*, Physical Review Letters, **71**(9) (1993), 1359–1362.

[6] W. Govaerts, Yu.A. Kuznetsov and B. Sijnave, *Bifurcations of maps in the software package* CONTENT, in "Computer Algebra in Scientific Computing — CASC'99" (eds.

V.G. Ganzha, E.W. Mayr and E.V. Vorozhtsov), Springer-Verlag, Berlin (1999), 191–206.

[7] C. Grebogi, E. Ott and J.A. Yorke, *Crises, sudden changes in chaotic attractors, and transient chaos*, Physica D, **7** (1983), 181–200.

[8] C. Grebogi, E. Ott and J.A. Yorke, *Metamorphoses of basin boundaries in nonlinear dynamical systems*, Physical Review Letters, **56**(10) (1986), 1011–1014.

[9] C. Grebogi, E. Ott and J.A. Yorke, *Basin boundary metamorphoses: Changes in accessible boundary orbits*, Physica D, **24** (1987), 243–262.

[10] M. Hénon, M., *A two-dimensional mapping with a strange attractor*, Communications in Mathematical Physics, **50** (1976), 69–77.

[11] S.M. Hammel, C.K.R.T. Jones and J.V. Moloney, *Global dynamical behaviour of the optical field in a ring cavity*, J. Optical Society of America B, **2**(4) (1985), 552–564.

[12] K. Ikeda, *Multiple-valued stationary state and its instability of the transmitted light by a ring cavity system*, Optics Communications, **30**(2) (1979), 257–261.

[13] K. Ikeda, H. Daido and O. Akimoto, *Optical turbulence: Chaotic behavior of transmitted light from a ring cavity*, Physical Review Letters, **45** (1980), 709–712.

[14] B. Krauskopf and H.M. Osinga, *Investigating torus bifurcations in the forced Van der Pol oscillator*, in "Numerical Methods for Bifurcation Problems and Large-Scale Dynamical Systems," (eds. E.J. Doedel and L.S. Tuckerman), IMA Vol. Math. Appl. **119**, Springer-Verlag, New York (2000), 199–208.

[15] C. Mira, J.-P. Carcassès, M. Bosch, C. Simó and J.C. Tatjer, *"Crossroad area-spring area" transition II. Foliated parametric representation*, Int. J. Bifurcation & Chaos **1**(2) (1991), 339–348.

[16] H.M. Osinga, *Locus of boundary crisis: Expect infinitely many gaps*, Physical Review E, 035201(R) (2006).

[17] H.M. Osinga, *Boundary crisis bifurcation in two parameters*, J. Differential Equations and Applications, **12**(10) (2006), 997–1008.

[18] J. Palis and F. Takens, "Hyperbolicity & Sensitive Chaotic Dynamics at Homoclinic Bifurcations," Cambridge studies in advanced mathematics **35**, Cambridge University Press, 1993.

[19] C. Simó, *On the Hénon–Pomeau attractor*, Journal of Statistical Physics, **21**(4) (1979), 465–494.

[20] E. Sander and J.A. Yorke, *Period-doubling cascades galore*, preprint, `arXiv:0903.3613`.

[21] E. Sander and J.A. Yorke, *The cascades route to chaos*, preprint, `arXiv:0910.3570`.

[22] Y. Ueda, *Randomly transitional phenomena in the system governed by Duffing's equation*, Journal of Statistical Physics, **20**(2) (1979) 181–196.

[23] Y. Ueda, *Explosion of strange attractors exhibited by Duffing's equations*, Annals of the New York Academy of Sciences, **357** (1980), 422–434.